iScience

CellPress
OPEN ACCESS

Article

Gold nanoparticles-anchored peptides enable precise colorimetric estimation of microplastics

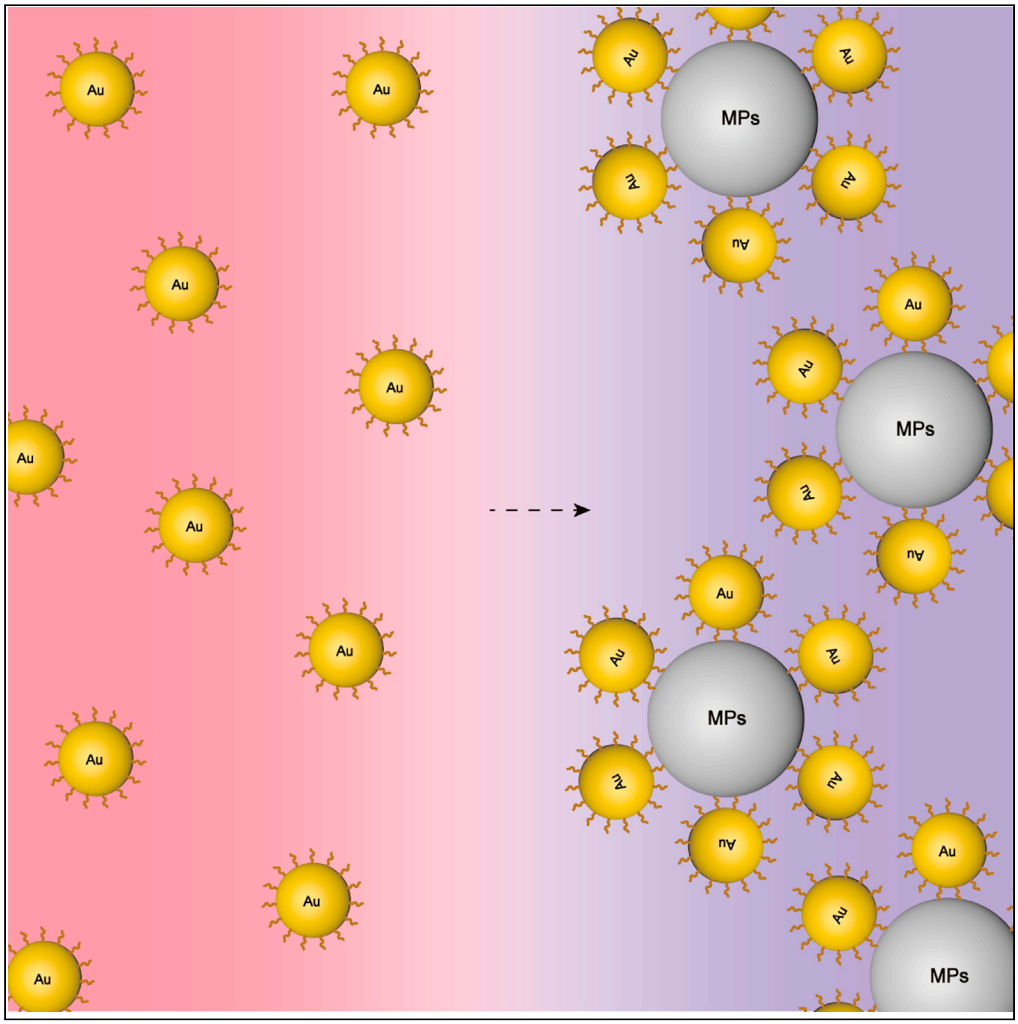

Jindi Zhao, Yongqiang Ruan, Zhe Zheng, ..., Fanghui Hu, Jiahuan Ling, Lihui Zhang

zhanglihui@njnu.edu.cn

Highlights

Gold nanoparticles (AuNPs)-anchored peptide (LCI/TA2) probes were constructed

Rapid and accurate detection of polypropylene or polystyrene microplastics was realized

The developed method is of great value in monitoring the microplastics pollution

Zhao et al., iScience 26, 106823
June 16, 2023
https://doi.org/10.1016/j.isci.2023.106823

iScience

CellPress
OPEN ACCESS

Article

Gold nanoparticles-anchored peptides enable precise colorimetric estimation of microplastics

Jindi Zhao,[1] Yongqiang Ruan,[1] Zhe Zheng,[1] Yunhan Li,[1] Muhammad Sohail,[1] Fanghui Hu,[1] Jiahuan Ling,[1] and Lihui Zhang[1,2,*]

SUMMARY

Microplastics (MPs, particle size < 5 mm) are an emerging contaminant in aquatic environment, which have attracted increasing attention worldwide. In this study, a colorimetric method for MPs detection was developed based on gold nanoparticles (AuNPs)-anchored peptides (LCI or TA2), which are able to specifically recognize and adhere to polypropylene (PP) or polystyrene (PS). The AuNPs-anchored peptides accumulated on the surface of MPs, rendering a color change from red to gray-blue and transforming the surface plasmon absorption intensity and wavelength. The designed method presented high selectivity, stability, and reproducibility, with a detection range of 2.5–15 μg/mL. The results demonstrated that the developed approach will be valuable in the precise, facile, and cost-effective estimation of MPs in different matrices, regulating the control over MPs pollution and its hazardous impact on health and ecosystems.

INTRODUCTION

The term "microplastics" (MPs) was first coined in 2004 to refer mainly to smaller pieces of debris,[1,2] but includes a much broader range at present. Polymers in the form of fibers, films, fragments, pellets, or particles with diameters ranging from 1 nm to 5 mm are considered MPs by the national oceanic and atmospheric administration.[3,4] Even if the world embarked immediately on a globally coordinated effort to reduce plastic consumption, there would still be 710 million metric tons of plastic by 2040.[5] Large plastic waste can be transformed into MPs by natural weathering, seawater erosion, ultraviolet irradiation, and biological effects. MPs, a type of persistent pollutant, are widely distributed in the environment and are difficult to degrade, with half-lives of hundreds of years.[6] In the second session of the United Nations Environment Assembly in 2015, MPs pollution was included as the second major scientific problem in the field of environmental and ecological sciences.

MPs were detected in many places, such as the Yellow Sea, the Three Gorges of the Yangtze River,[7] and Taihu Lake.[8] Kosuth et al.[9] studied the content of MPs in tap water and estimated that the average annual intake of MPs in the human body was more than 5,800, of which about 88% came from tap water. Since MPs are widespread in the water environment and are able to cause serious harm to human health through the food chain, monitoring the content of MPs in water (drinking water, oceans, lakes, etc.) is crucial for environmental analysis and water safety. In order to detect the MPs in water, a series of detection methods have been developed. Conventional methods for the determination of MPs in water samples include pyrolysis gas chromatography,[10] Fourier transform infrared spectroscopy,[11] Raman spectroscopy,[12] etc. Although these methods exhibit high selectivity and sensitivity, they are costly, labor-intensive, and time-consuming.

Gold nanoparticles (AuNPs) are ideal nanomaterials for optical biosensing because of their high molar extinction coefficient, large specific surface area, and good biocompatibility, and their optical properties are related to shape, size, and distance distribution.[13] AuNPs typically bind to biomolecules (such as nucleic acids, proteins, peptides, etc.) to form complexes with different properties. When these complexes are combined with the test objects, detection results with high sensitivity and accuracy can be obtained by using simple instruments, such as an ultraviolet (UV) spectrophotometer.[14] The composite not only possesses the unique features of biomolecules but also owns the optical, electrical, magnetic and catalytic properties of AuNPs. The diversity of the polypeptide structure and its high biological activity make it

[1]School of Food Science and Pharmaceutical Engineering, Nanjing Normal University, Nanjing 210046, China

[2]Lead contact

*Correspondence: zhanglihui@njnu.edu.cn

https://doi.org/10.1016/j.isci.2023.106823

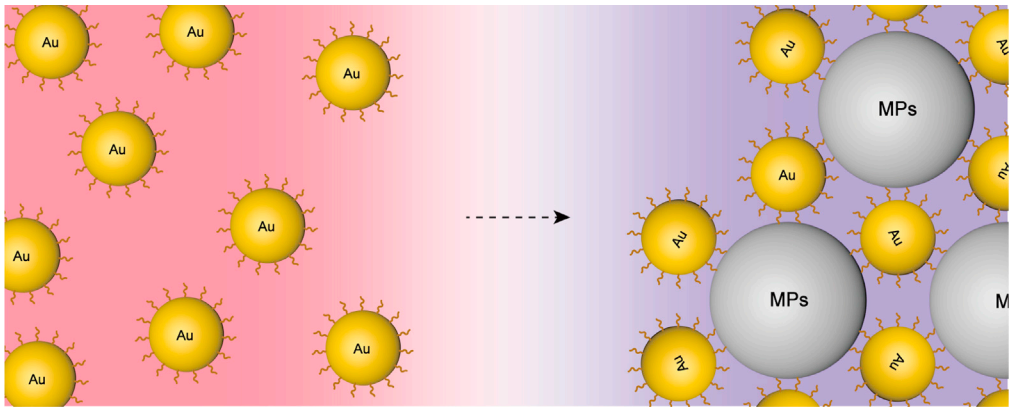

Scheme 1. Schematic illustrations of colorimetric sensing mechanism
The paper based on microplastics (MPs)-induced aggregation of peptide-conjugated gold nanoparticles (AuNPs).

more suitable to synthesize the composite with AuNPs for the analysis and detection of the target analytes. Parnsubsakul et al.[15] designed the polypeptide EKEKEKPPPPC and constructed a nickel ion colorimetric sensor based on the EKEKEKPPPPC-AuNPs complex with the help of the high affinity between the polypeptide and nickel ions. Hiroshi and colleagues[16] reported a lectin sensing strategy based on a polypeptide-gold nanoparticle carbohydrate complex. In recent years, polypeptide-AuNPs complexes have shown promising applications in the field of biosensing. However, it is rarely used in the detection of MPs. The anchored peptide liquid chromatography peak I (LCI) has β Folded structure, stable in an aqueous solution. Polypropylene (PP) surface is hydrophobic, and the interaction with peptide LCI is mainly controlled by hydrophobic interaction.[17] Tachystatin A2 (TA2) was reported to be enriched in aromatic amino acids and the side group of the polystyrene (PS) macromolecular chain is the benzene ring. The binding mechanism of the aromatic amino acids of TA2 and the aromatic moieties of PS is primarily based upon the stacking of aromatic ring systems.[18–20] This means that the anchoring peptides LCI and TA2 can bind to PP and PS, respectively.

To circumvent the drawbacks of the available MPs detection approaches, such as a high detection limit, low sensitivity, high cost, labor-intensive, and time-consuming, we fabricated a colorimetric method for the estimation of MPs using AuNPs-anchored peptides (LCI or TA2) with specific recognition and adhesion to MPs. In principle, the AuNPs-anchored peptides accumulated on the surface of MPs, rendering a color change from red to gray-blue and transforming the surface plasmon resonance absorption intensity and wavelength. At present, AuNPs combined with peptides have not been studied in the detection of MPs. Therefore, our project aimed to explore the specific recognition and detection of MPs using AuNPs-anchored peptide, facilitating the commercial detection and control over MPs pollution.

RESULTS AND DISCUSSION

Principles of MPs detection

The amino groups of the N-terminals of the anchored peptides LCI and TA2 (the sequences are shown in Table S1) were conjugated to the carboxyl group on the surface-modified AuNPs via an amide linkage. Theoretically, in an alkaline environment, AuNPs-LCI (pI = 5.43) and AuNPs-TA2 (pI = 5.13) are more stable than AuNPs because the anchored peptides are negatively charged and form a uniform layer, increasing the electrostatic repulsion between AuNPs.[21] In addition, LC1 and TA2 can attach specifically to the surfaces of MPs, PP, and PS, through hydrophobic interactions,[17] further inducing the aggregation of AuNPs, Scheme 1.

Anchor peptides bind specifically to MPs

To justify the specific binding of anchored peptides and MPs, the EGFP was introduced into the anchored peptide structure and was combined with EGFP anchored peptide and interval sequence (10 alanine and tobacco etch virus [TEV] protease cleavage sites) to form a fusion protein, as shown in

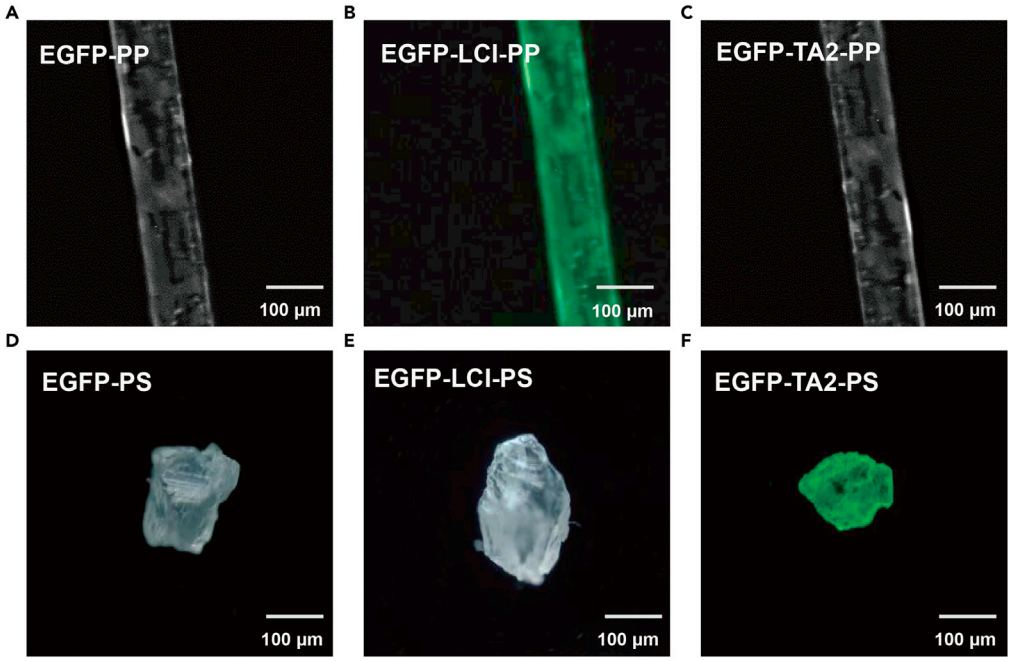

Figure 1. Binding of EGFP-anchored peptide fusion proteins to polypropylene (PP) and polystyrene (PS) surfaces

(A) EGFP protein to PP fiber surfaces (EGFP-PP).

(B) EGFP-LCI fusion protein to PP fiber surface (EGFP-LCI-PP).

(C) EGFP-TA2 fusion protein to PP fiber surface (EGFP-TA2-PP).

(D) EGFP protein to the surface of PS particles (EGFP-PS).

(E) EGFP-LCI fusion protein to the surface of PS particles (EGFP-LCI-PS).

(F) EGFP-TA2 fusion protein to the surface of PS particles (EGFP-TA2-PS). The EGFP and the fusion proteins, EGFP-LCI and EGFP-TA2 were used as negative and positive controls, respectively. (scale bar = 100 μm).

Figure S1A. The sodium dodecyl sulfate polyacrylamide gel electrophoresis (SDS-PAGE) verified the normal expression of the fusion protein, as shown in Figure S1B. Fluorescence microscope images showed that EGFP, as a positive control, did not affect the binding of anchored peptides and plastic. The LCI and TA2 specifically interacted with PP and PS, respectively, as shown in Figure 1.

AuNPs bind to anchored peptides

The absorption peak of AuNPs is generally in the range of 500–600 nm, and the UV-PC1800 spectra showed that the absorption peak of AuNPs synthesized in this experiment was 535 nm. The stability of AuNPs was extremely important in the testing process; hence, AuNPs were placed at 4°C for one month and tested for stability. The results showed that the absorption peak of the AuNPs did not change significantly after being placed at 4°C for one month, as shown in Figure 2A, indicating that AuNPs had good stability and were suitable for the detection of MPs. In addition, the shape of the absorption peak was symmetrical, demonstrating that the AuNPs were of uniform particle size.[22] Furthermore, TEM analysis was performed to verify the correlation between UV-PC1800 spectral analysis and AuNPs morphology. As shown in Figure 2A, AuNPs were spherical with a uniform size distribution and good dispersibility. In addition, as shown in Figure S2, the particle size distribution of AuNPs is mainly around 30 nm.

Peptides have become a core material for the surface modification of nanomaterials due to their good biocompatibility and facile modifications. Peptides can be modified on the surface of materials in both covalent and non-covalent ways, and the modified materials can be used for the detection of various substances.[15,23] In this study, amino groups were present in the anchored peptide (as shown in Figure 2B), and the modification process was realized by forming an amide bond between amino groups in the anchored peptide and carboxyl groups in the modified AuNPs. To modify AuNPs with anchored peptides,

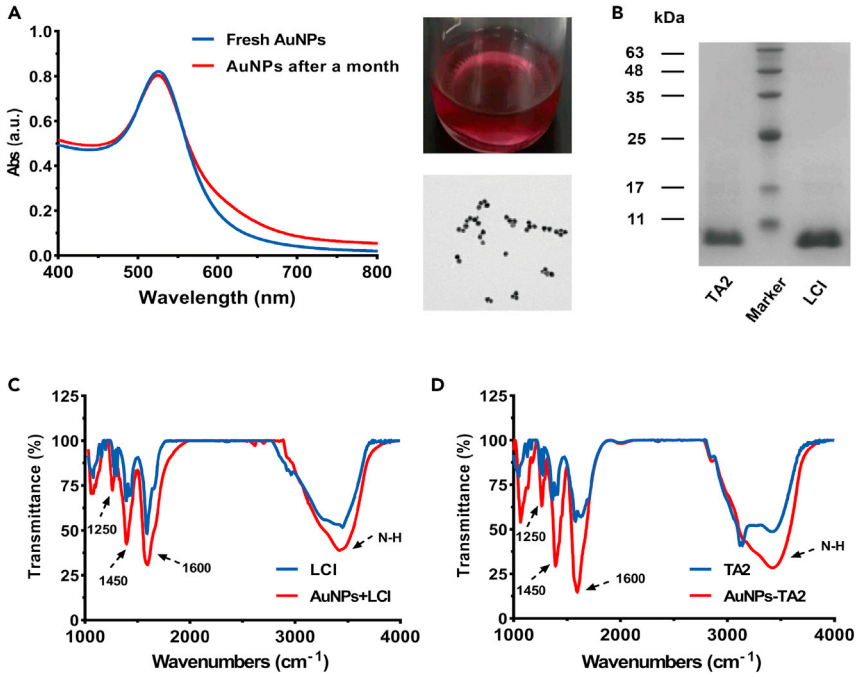

Figure 2. AuNPs bound to the anchored peptides

(A) AuNPs stability and SEM images of AuNPs.

(B) Purification of the anchored peptides LCI and TA2.

(C) FTIR of AuNPs bound to the anchored peptide LCI.

(D) FTIR of AuNPs bound to anchored peptide TA2.

thiol-containing undecanoic acid was assembled on the AuNPs surface by AU-S bond to form a monolayer so that carboxyl groups were obtained on the surface of AuNPs. In this case, the anchored peptides were modified on the surface of AuNPs by covalent bonding, as shown in Figures 2C and 2D. It can be seen that the FTIR spectra of AuNPs modified with anchored peptides were consistent with those of pure anchored peptides. The characteristic bands of anchored peptides, such as the amide I band at 1600 cm^{-1}, the amide II band at 1450 cm^{-1}, and the amide III band at 1250 cm^{-1}, were completely retained in the infrared spectra of AuNPs. Therefore, it can be inferred that the backbone and functional groups of the anchored peptide chain remained intact after binding of the anchored peptide to the AuNPs. Based on the FTIR results, we speculated that the anchored peptide binding and AuNPs remained bioactive.

In addition, as shown in Figure S3, The zeta potential of AuNPs (−44 mV) has no significant difference from that of AuNPs-LCI (−40 mV) and AuNPs-TA2 (−42 mV), indicating that the LCI or TA2 modification has no significant effect on the stability of AuNPs.

MPs induce aggregation of AuNPs-anchored peptide

To demonstrate the binding effect of AuNPs-anchored peptide and MPs, UV spectra of AuNPs, anchored peptide, MPs, AuNPs-anchored peptide, AuNPs-MPs, and AuNPs-anchored peptide-MPs were obtained, as shown in Figures 3A and 3B. The AuNPs presented an absorption peak at about 535 nm, while the AuNPs modified with anchoring peptides generated symmetrical absorption peaks at 570 nm and 567 nm. The results showed that the anchored peptides were successfully conjugated on the surface of AuNPs, and the AuNPs-anchored peptide complex offered good dispersibility in solution. The presence of MPs in the reaction matrix decreased the value of the absorption peak of the AuNPs-anchored peptide system to 0.42 and 0.49. There was no obvious absorption peak in the UV absorption spectra of the anchored peptide, MPs, and anchored peptide-MPs, and the absorption peak of AuNPs-MPs was consistent with that of AuNPs. In addition, the absorption peaks of AuNPs-LCI-PP + PS and AuNPs-LCI-PP, AuNPs-TA2-PP+PS, and AuNPs-TA2-PS did not show obvious changes, as shown in Figure S4. In conclusion, the MPs interacted

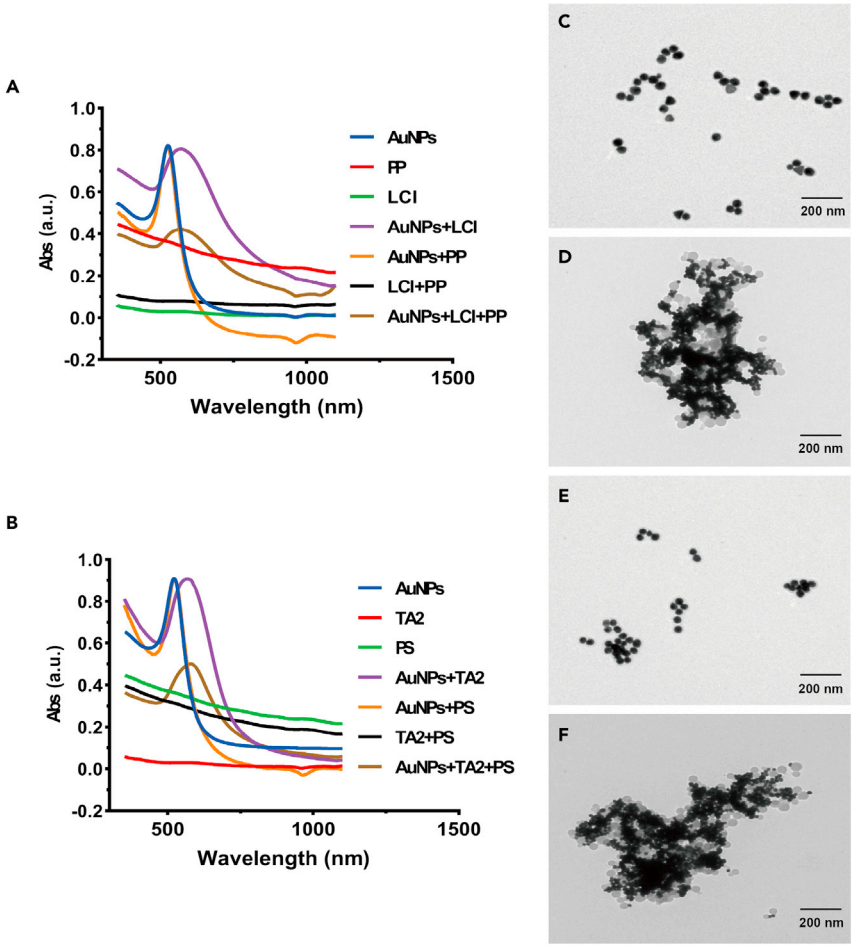

Figure 3. Spectral analysis and characterization of AuNPs-anchored peptide aggregation induced by MPs

(A) Ultraviolet-visible absorption spectra of PP.

(B) Ultraviolet-visible absorption spectra of PS.

(C) TEM image of AuNPs-LCI.

(D) TEM image of AuNPs-LCI-PP.

(E) TEM image of AuNPs-TA2.

(F) TEM image of AuNPs-TA2-PS. (scale bar = 200 nm).

with AuNPs-anchored peptide molecules and changed the absorption traits of the AuNPs-anchored peptide system, enabling the detection of MPs.

Moreover, transmission electron microscope (TEM) analysis was performed to further elaborate the interaction between the AuNPs-anchored peptide and MPs. The TEM images in Figures 3C and 3D showed that the AuNPs-anchored peptide had good dispersibility. Besides, AuNPs-anchored peptide molecules aggregated in the presence of MPs, as shown in Figures 3E and 3F.

Parameters optimization

The maximum output of a reaction system is directly related to the principle of parameter optimization; hence, various parameters, including the anchored peptide concentration, reaction pH, and mixing time, were optimized. The size of the AuNPs and the concentration of the anchored peptides were optimized, and the ratios of A_{750}/A_{570} and A_{800}/A_{567} reached maximum when the average size of AuNPs was 30 nm and the anchored peptide concentration was 2.5 mg/mL in the presence of MPs, as shown in Figure 4. In addition, the pH value of the solution also played a critical role. When the pH of the solution was below the pI of the anchored peptide, the anchored peptide had a positive charge and caused the aggregation of

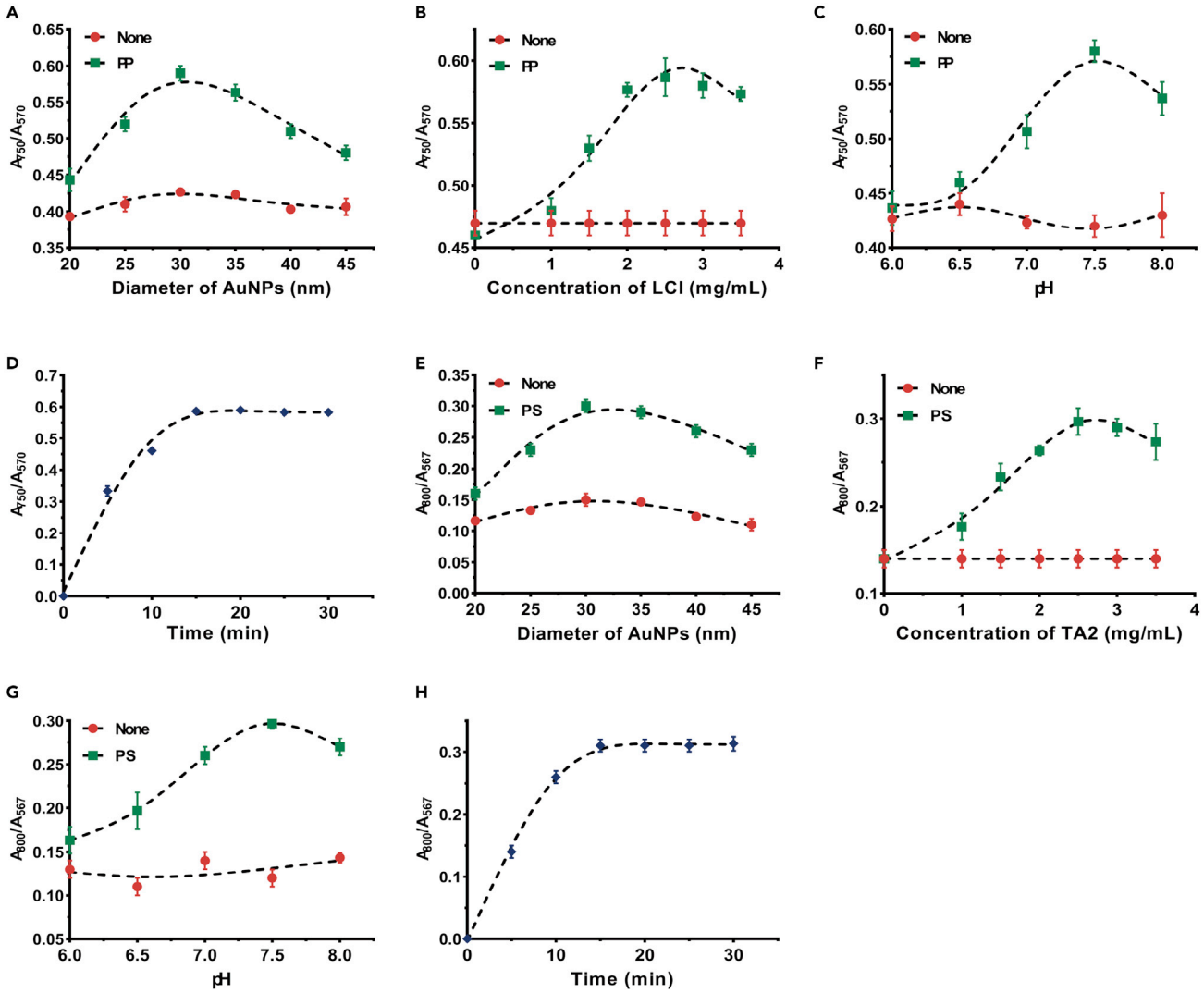

Figure 4. Parameters optimization

(A) Effect of the diameter of AuNPs.

(B) The concentration of LCl.

(C) The pH of the AuNPs-LCl system.

(D) The reaction time of AuNPs-LCl and PP.

(E) Effect of the diameter of AuNPs.

(F) The concentration of TA2.

(G) The pH of the AuNPs-TA2 system.

(H) The reaction time of AuNPs-TA2 and PS. Results are presented as mean ± SD (n = 3).

AuNPs. However, in an alkaline environment, the negatively charged anchored peptide formed a uniform charged layer, which increased the electrostatic repulsion between AuNPs. It can be seen from Figures 4C and 4G that the most appropriate pH was 7.4. Under the above-mentioned optimal conditions, the influence of reaction time on the system was also studied. It can be observed from Figures 4D and 4H that the values of A_{750}/A_{570} and A_{800}/A_{567} increased gradually with time and stabilized after 15 min, indicating that the reaction had been at equilibrium state.

Colorimetric assay for rapid MPs sensing

We prepared 2.5–15 μg/mL PP and PS suspensions in water. The color of the AuNPs gradually changed from red to purple and finally to blue-gray as the MPs concentration was increased, Figures S5A and

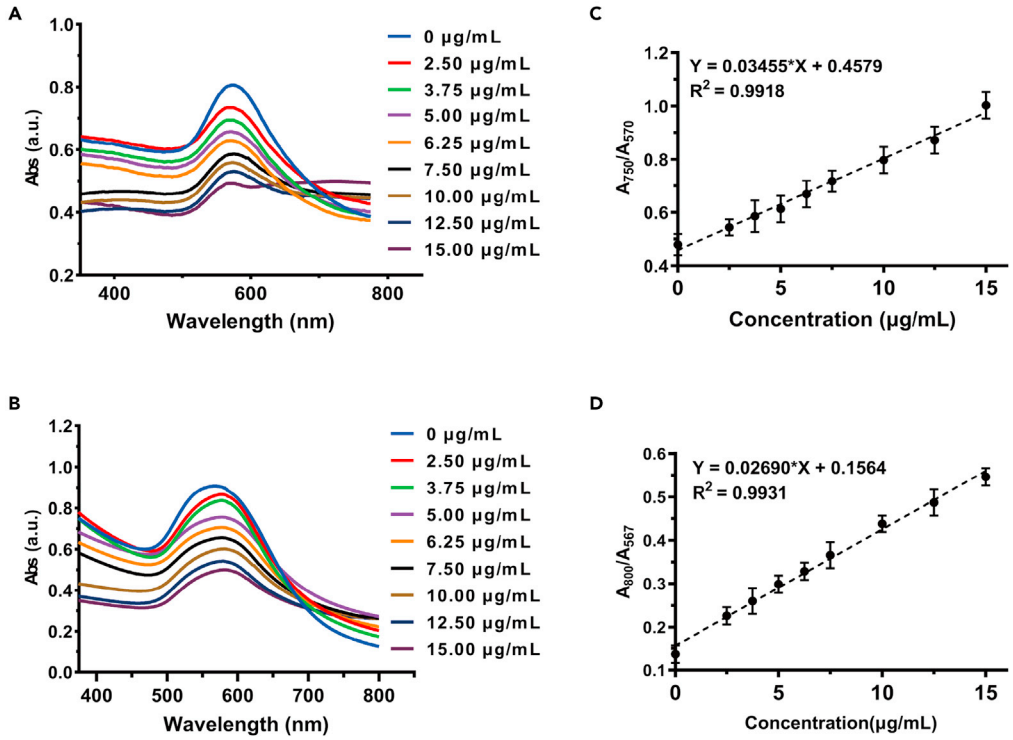

Figure 5. Quantitative characterization of MPs

(A) UV-Vis spectra of AuNPs-LCI with different concentrations of PP.

(B) UV-Vis spectra of AuNPs-TA2 after adding different concentrations of PS.

(C) Absorption ratios (A_{750}/A_{570}) of AuNPs-LCI with different concentrations of PP.

(D) Absorption ratios (A_{800}/A_{567}) of AuNPs-TA2 with different concentrations of PS. Results are presented as mean ± SD (n = 3).

S5B, and the intensities of absorption peaks at 570 nm and 567 nm decreased gradually, Figures 5A and 5B. These results indicated that the aggregation of AuNPs-anchored peptides depended on the concentration of MPs. We used the ratio of absorptions (A_{750}/A_{570} and A_{800}/A_{567}) to express the degree of aggregation as mentioned above. Figure 5C showed that the concentration of PP relied on the colorimetric response (A_{750}/A_{570} values) of the assay. The A_{750}/A_{570} values increased linearly with the PP concentration in the range of 2.5–15 μg/mL, and the linear regression correlation coefficient was 0.9918. Figure 5D showed that the response of the A_{800}/A_{567} assay was linear, with a linear regression correlation coefficient of 0.9931, at the PS concentration range of 2.5–15 μg/mL. The values of regression correlation coefficients were close to 1, indicating that our new method was sensitive to the detection of MPs.[21]

Selectivity for determination of MPs

Other MPs may interfere with the detection of PP and PS, so we selected some common MPs, such as PS, PVC, PS, PET, PE, and PP. Under optimized conditions, the AuNPs-LCI system presented a much higher value of A_{750}/A_{570} in the presence of PP as compared to the other MPs, Figure 6A. In addition, the A_{800}/A_{567} ratio of MPs in the presence of PS in the AuNPs-TA2 system was much higher than that of other MPs, as shown in Figure 6B. Besides, the colorimetric method demonstrated significant selectivity for PP and PS, as shown in Figures S5C and S5D. The above results indicated that the two detection systems had good selectivity for the monitoring of PP and PS.

Detection of actual water sample

To validate the accuracy and sensitivity of this method, we applied the fabricated method to the real environmental samples. MPs may exist in some environmental samples, such as lake water or tap water, so the samples were collected from the lake water of Nanjing Normal University. The samples were tested using the traditional Raman method, and no MPs were detected, as shown in Figure S6. Therefore, we added

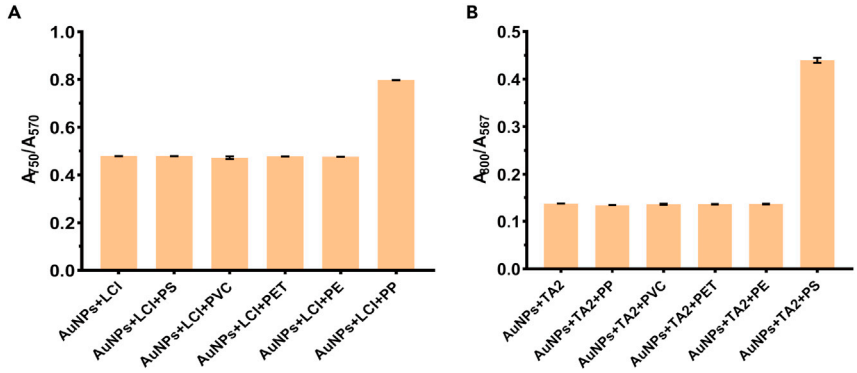

Figure 6. Selectivity for the determination of MPs

(A) PS, PVC, PS, PET, PE, and PP were added into the AuNPs-LCI system.

(B) PP, PVC, PET, PE, and PS were added into the AuNPs-TA2 system. Results are presented as mean ± SD (n = 3).

different concentrations of PP and PS (3.75, 7.5, and 12.5 μg/mL) to the lake water. The recovery results of MPs in the spiked lake water samples were shown in Table 1 and Table 2. The PP recovery of this method was within the range of 92.50–99.47%, and the relative standard deviation was between 1.52 and 2.07%. The PS recovery of this method was within the range of 96.57–110%, and the relative standard deviation was between 1.52 and 2.39%. The results showed that the designed colorimetric method could be used to detect MPs in real water samples. In addition, Table S2 gives several commonly used methods for the detection of microplastics at present. It can be seen that this experimental method has the advantages of time saving, labor-saving, and low detection limit. Therefore, it is worthwhile to develop anchoring peptides that specifically recognize other MPs in the future.

Conclusions

In conclusion, we presented a rapid and simple method for the detection of MPs using MPs as aggregation promoters for AuNPs-anchored peptides. To the best of our knowledge, there are few reports on the detection of MPs using the interaction between anchored peptides and MPs. The detection results were highly linear, and the reaction was completed within 15 min. Besides, anchored peptides (LCI or TA2) rendered the detection system specific for the precise detection of MPs. Briefly, the results demonstrated that the developed approach will be valuable in the precise, facile, and cost-effective estimation of MPs in different matrices, regulating the control over MP pollution and its hazardous impact on health and ecosystems.

Limitations of the study

This proposed methodology has still many limitations to apply for other plastics, various sizes, and media types. Nevertheless, we hope that this suggestion will give rise to a new measurement method that can be used to measure various sizes and types of microplastics in the future.

STAR★METHODS

Detailed methods are provided in the online version of this paper and include the following:

- KEY RESOURCES TABLE
- RESOURCE AVAILABILITY

Table 1. Results of PP (polypropylene) recovery experiments performed in the spiked lake water samples

Sample (lake water)	Content (Raman detection)	PP (added) μg/mL	PP (detected) μg/mL	Recovery (%)	RSD (%)
1	ND	3.75	3.73	99.47%	1.52%
2	ND	7.5	6.94	92.50%	2.07%
3	ND	12.5	11.83	94.68%	1.55%

n.d.: not detected, Results are presented as mean ± SD (n = 3).

Table 2. Results of PS (polystyrene) recovery experiments performed in the spiked lake water samples

Sample (lake water)	Content (Raman detection)	PS (added) μg/mL	PS (detected) μg/mL	Recovery (%)	RSD (%)
1	ND	3.75	4.13	110%	2.39%
2	ND	7.5	7.95	106%	2.50%
3	ND	12.5	12.07	96.57%	1.52%

n.d.: not detected, Results are presented as mean ± SD (n = 3).

SUPPLEMENTAL INFORMATION

Supplemental information can be found online at https://doi.org/10.1016/j.isci.2023.106823.

ACKNOWLEDGMENTS

This work was financially supported by the National Key Research and Development Program of China (No. 2019YFA0706900) and the Natural Science Fund for Colleges and Universities in Jiangsu Province (No. 22KJB530008).

AUTHOR CONTRIBUTIONS

J.Z. proposed research ideas, designed research schemes, analyzed data, and wrote the first draft of this paper. Y.R. analyzed data. J.Z. and Z.Z. carried out the experiments. Y.L., M.S., F.H., and J.L. revised the manuscript. L.Z. revised and finalized the manuscript.

DECLARATION OF INTERESTS

The authors declare no competing interests.

Received: March 8, 2023
Revised: April 12, 2023
Accepted: April 24, 2023
Published: May 8, 2023

REFERENCES

1. Shabbir, S., Faheem, M., Ali, N., Kerr, P.G., Wang, L.F., Kuppusamy, S., and Li, Y. (2020). Periphytic biofilm: an innovative approach for biodegradation of microplastics. Sci. Total Environ. *717*, 137064. https://doi.org/10.1016/j.scitotenv.2020.137064.

2. Rivoira, L., Castiglioni, M., Rodrigues, S.M., Freitas, V., Bruzzoniti, M.C., Ramos, S., and Almeida, C.M.R. (2020). Microplastic in marine environment: reworking and optimisation of two analytical protocols for the extraction of microplastics from sediments and oysters. MethodsX *7*, 101116. https://doi.org/10.1016/j.mex.2020.101116.

3. Diaz-Basantes, M.F., Conesa, J.A., and Fullana, A. (2020). Microplastics in honey, beer, milk and refreshments in Ecuador as emerging contaminants. Sustainability *12*, 5514. https://doi.org/10.3390/su12145514.

4. Li, Z., Li, Q., Li, R., Zhao, Y., Geng, J., and Wang, G. (2020). Physiological responses of lettuce (Lactuca sativa L.) to microplastic pollution. Environ. Sci. Pollut. Res. Int. *27*, 30306–30314. https://doi.org/10.1007/s11356-020-09349-0.

5. Amelia, T.S.M., Khalik, W.M.A.W.M., Ong, M.C., Shao, Y.T., Pan, H.-J., and Bhubalan, K. (2021). Marine microplastics as vectors of major ocean pollutants and its hazards to the marine ecosystem and humans. Prog. Earth Planet. Sci. *8*, 12. https://doi.org/10.1186/s40645-020-00405-4.

6. Lozano, Y.M., and Rillig, M.C. (2020). Effects of microplastic fibers and drought on plant communities. Environ. Sci. Technol. *54*, 6166–

6173. https://doi.org/10.1021/acs.est.0c01051.

7. Zhang, K., Gong, W., Lv, J., Xiong, X., and Wu, C. (2015). Accumulation of floating microplastics behind the three gorges dam. Environ. Pollut. *204*, 117–123. https://doi.org/10.1016/j.envpol.2015.04.023.

8. Su, L., Xue, Y., Li, L., Yang, D., Kolandhasamy, P., Li, D., and Shi, H. (2016). Microplastics in Taihu lake, china. Environ. Pollut. *216*, 711–719. https://doi.org/10.1016/j.envpol.2016.06.036.

9. Kosuth, M., Mason, S.A., and Wattenberg, E.V. (2018). Anthropogenic contamination of tap water, beer, and sea salt. PLoS One *13*, e0194970. https://doi.org/10.1371/journal.pone.0194970.

10. Funck, M., Yildirim, A., Nickel, C., Schram, J., Schmidt, T.C., and Tuerk, J. (2020). Identification of microplastics in wastewater after cascade filtration using Pyrolysis-GC-MS. MethodsX *7*, 100778. https://doi.org/10.1016/j.mex.2019.100778.

11. Turner, A., and Holmes, L. (2011). Occurrence, distribution and characteristics of beached plastic production pellets on the island of Malta (central Mediterranean). Mar. Pollut. Bull. *62*, 377–381. https://doi.org/10.1016/j.marpolbul.2010.09.027.

12. Collard, F., Gilbert, B., Eppe, G., Parmentier, E., and Das, K. (2015). Detection of anthropogenic particles in fish stomachs: an isolation method adapted to identification by Raman spectroscopy. Arch. Environ. Contam. Toxicol. *69*, 331–339. https://doi.org/10.1007/s00244-015-0221-0.

13. Sathiyaraj, S., Suriyakala, G., Gandhi, A.D., Babujanarthanam, R., Almaary, K.S., and Chen, T.W. (2020). Synthesis, characterization, and antibacterial activity of biosynthesized gold nanoparticles. Biointerface Research in Applied Chemistry *11*, 9619–9628. https://doi.org/10.33263/briac112.96199628.

14. Chen, H., Huang, J., Palaniappan, A., Wang, Y., Liedberg, B., Platt, M., and Tok, A.I.Y. (2016). A review on electronic bio-sensing approaches based on non-antibody recognition elements. Analyst *141*, 2335–2346. https://doi.org/10.1039/c5an02623g.

15. Parnsubsakul, A., Oaew, S., and Surareungchai, W. (2018). Zwitterionic peptide-capped gold nanoparticles for colorimetric detection of Ni(2+). Nanoscale *10*, 5466–5473. https://doi.org/10.1039/c7nr07998b.

16. Tsutsumi, H., Shirai, T., Ohkusa, H., and Mihara, H. (2018). Gold nanoparticles conjugated with glycopeptides for lectin detection and imaging on cell surface. Protein Pept. Lett. *25*, 84–89. https://doi.org/10.2174/0929866525666171218124434.

17. Rübsam, K., Davari, M.D., Jakob, F., and Schwaneberg, U. (2018). KnowVolution of the polymer-binding peptide LCI for improved polypropylene binding. Polymers *10*, 423. https://doi.org/10.3390/polym10040423.

18. Serizawa, T., Matsuno, H., and Sawada, T. (2011). Specific interfaces between synthetic polymers and biologically identified peptides. J. Mater. Chem. *21*, 10252–10260. https://doi.org/10.1039/c1jm10602c.

19. Adey, N.B., Mataragnon, A.H., Rider, J.E., Carter, J.M., and Kay, B.K. (1995). Characterization of phage that bind plastic from phage-displayed random peptide libraries. Gene *156*, 27–31. https://doi.org/10.1016/0378-1119(95)00058-e.

20. Menendez, A., and Scott, J.K. (2005). The nature of target-unrelated peptides recovered in the screening of phage-displayed random peptide libraries with antibodies. Anal. Biochem. *336*, 145–157. https://doi.org/10.1016/J.AB.2004.09.048.

21. Li, X., Wu, Z., Zhou, X., and Hu, J. (2017). Colorimetric response of peptide modified gold nanoparticles: an original assay for ultrasensitive silver detection. Biosens. Bioelectron. *92*, 496–501. https://doi.org/10.1016/j.bios.2016.10.075.

22. Ren, Y., Wei, J., He, Y., Wang, Y., Bai, M., Zhang, C., Luo, L., Wang, J., and Wang, Y. (2021). Ultrasensitive label-free immunochromatographic strip sensor for Salmonella determination based on salt-induced aggregated gold nanoparticles. Food Chem. *343*, 128518. https://doi.org/10.1016/j.foodchem.2020.128518.

23. Li, X.Y., Feng, F.Y., Zhou, X.D., and Hu, J.M. (2018). Rational design of an anchoring peptide for high-efficiency and quantitative modification of peptides and DNA strands on gold nanoparticles. Nanoscale *10*, 11491–11497. https://doi.org/10.1039/c8nr03565b.

STAR★METHODS

KEY RESOURCES TABLE

REAGENT or RESOURCE	SOURCE	IDENTIFIER
Chemicals, peptides, and recombinant proteins		
Sodium citrate	Macklin	CAS: 68-04-2
Chloroauric acid	Macklin	CAS: 16903-35-8
11-mercaptodecanoic acid	Macklin	CAS: 71310-21-9
N-Hydroxy succinimide (NHS)	Macklin	CAS: 6066-82-6
1-(3-Dimethylaminopropyl)-3-ethylcarbodiimide (EDC)	Macklin	CAS: 1892-57-5
Tobacco etch virus (TEV) protease	Beyotime	Cat#P2307
Polypropylene (PP)	Taobao	N/A
Polyethylene(PE)	Taobao	N/A
Polyvinyl chloride (PVC)	Taobao	N/A
Polystyrene (PS)	Taobao	N/A
Polyethylene terephthalate (PET)	Taobao	N/A

RESOURCE AVAILABILITY

Lead contact

Further information and requests for resources should be directed to and will be fulfilled by the lead contact, Prof. Lihui Zhang (zhanglihui@njnu.edu.cn).

Materials availability

This study did not generate new unique reagents. All chemicals were obtained from commercial resources and used as received.

Data and code availability

- All data reported in this paper will be shared by the lead contact upon request.
- This paper does not report original code.
- Any additional information required to reanalyze the data reported in this paper are available from the lead contact upon request.

METHOD DETAILS

Synthesis and modification of AuNPs

Firstly, 20 mL of 0.01% chloroauric acid was added to a 50-mL round-bottom flask with a magneton, fitted with a spherical condensing tube, and heated to boiling. After that, 2 mL of the 1% sodium citrate solution was added at once to the boiling mixture, and vigorous stirring was continued during reflux for 10 min. Heat source was turned off mixture was stirred for another 15 min and cooled to room temperature.

The suspension of AuNPs (0.05 mg/mL, 25 mL) was mixed with the solution of 11-mercaptoundecanoic acid (10 mM, 25 mL) in a 50-mL centrifuge tube and placed at 4°C for 12 h. Then, the suspension was centrifuged at 8000 rpm for 1 h, and the supernatant, which contained unreacted 11-mercaptoundecanoic acid, was removed to get the surface-functionalized AuNPs.

Construction and expression of recombinant plasmids

The plasmid pET28a (+): anchoring peptide was synthesized as the vector skeleton of the fusion protein. The vector backbone pET28a (+): anchoring peptide was amplified using F-vector and R-vector, and the primers F-EGFP and R-EGFP were used to amplify the EGFP fragment. Linearized vectors and inserted

fragments were cloned and converted to DH5α by thermal shock. The positive clones were screened by PCR and sequenced by Nanjing Tsingke. The plasmids extracted from the positive clones and verified by sequencing were transformed into *E. coli* BL21 (DE3). Single colonies were selected and cultured in Luria-Bertani (LB) media containing Kana. Isopropyl β-D-Thiogalactoside (IPTG) with a final concentration of 0.1 mM was added to induce protein overexpression at 20°C. Cells were disintegrated by ultrasound and the supernatant was collected. The EGFP-anchored peptide fusion protein was purified by His gravity column (Takara, Beijing, China), dialysis, and ultrafiltration. The concentration of the protein was determined by the BCA kit and UV-Vis spectroscopy, and the expression of the recombinant protein was detected by SDS-PAGE using 5% concentrated glue and 12% separated glue.

EGFP-anchored peptide fusion protein binds to the surface of MPs

The PP fibers and PS particles were added to 2 mL solution of EGFP-fusion protein and EGFP protein, and they were allowed to react for 10 min at room temperature. Then the suspension was washed thrice with 10 mL portions of Tris/HCl buffer. Finally, they were observed under a fluorescence microscope (Olympus, Beijing, China).

Synthesis and identification of AuNPs-anchored peptide

The EGFP-fusion protein was cleaved by the tobacco etch virus (TEV) protease, which specifically recognized the amino acid sequences of Glu-Asn-Leu-Tyr-Phe-Gln-Gly and precisely cleaved the fusion protein into EGFP and the anchor peptide. Then the lysate was transferred to His gravity column (Takara, Beijing, China), and the anchored peptide was collected in circulation. The anchored peptide was dissolved in PB solution (pH 7.4) to a concentration of 10 mM for further use.

The 11-mercaptoundecanoic acid-modified AuNPs (3 mL) were mixed with 50 μL of anchor peptide and 50 μL of EDC-NHS mixture and allowed to react at 4°C for 24 h. The unreacted anchor peptide was removed by centrifugation (9500 rpm, 25 min) and washing thrice.

AuNPs and AuNPs-anchored peptides were analyzed by Fourier transform infrared spectroscopy (FTIR) (Vertex 70, Bruck, Germany). The absorbance in the mid-infrared region of 4000-400 cm^{-1} was measured with a scanning resolution of 4 cm^{-1}. The background absorbance was measured and subtracted from the tested samples.

The surface zeta potential of AuNPs and AuNPs-anchored peptides in solution was tested using a dynamic light scattering particle size distribution instrument (Zeta PALS, BIC, America).

Colorimetric detection of MPs

PP/PS solutions with different concentrations (2.5-15 μg/mL) were prepared. The AuNPs-anchored peptide complex (3 mL) was evenly mixed with MPs solutions of different gradient quantities and incubated at 4°C for 15 min. After incubation, color changes were observed, and the UV-Vis spectra of the reaction mixture were recorded. In the AuNPs-LCI system, the absorption values at 570 nm and 750 nm corresponded to the number of dispersed and aggregated AuNPs, respectively. Therefore, the relationship of dispersed to aggregated AuNPs could be described by the ratio of the absorption value at 750 nm to the absorption value at 570 nm (A_{750}/A_{570}). In the AuNPs-TA2 system, the absorption values at 567 nm and 800 nm belonged to the number of dispersed and aggregated AuNPs, respectively. Therefore, the ratio of dispersed to aggregated AuNPs could be represented by the ratio of absorption values at 800 nm to those at 567 nm (A_{800}/A_{567}), respectively.

Selectivity and recovery test for MPs

The same method was used in the selectivity experiments. We prepared suspensions of common MPs (such as Polyethylene (PE), Polyvinylchloride (PVC), Polyethylene terephthalate (PET), PS and PP) with equivalent concentrations and added them to the solution of AuNPs-anchored peptide. The reaction solution was characterized by the UV-Vis spectrophotometer (1800PC, Shanghai, China).

The recovery experiments were accomplished using MPs-spiked Lake water. Compared with the standard curve of MPs, we confirmed the PP and PS concentration in the samples by using the responses (A_{750}/A_{570} and A_{800}/A_{567}) of the colorimetric assay against MPs-spiked water samples. Raman's method was used for

the analysis of lake water without MPs-spiking. A portable Raman spectrometer (Prosp-Micro-S1, Hangzhou, China) with 785 nm excitation light was used to collect SERS signals. The laser power was about 105 mW and the exposure time for each SERS amount was 3 s.

QUANTIFICATION AND STATISTICAL ANALYSIS

All the experiments were performed in triplicates with the results presented as a mean value with standard deviation (Mean $\pm$ SD). The data were analyzed using analysis of variance, and the significant difference between the means was compared using *t*-test at a significance level at $p < 0.050$. Statistical analysis was done using Statistical Processor System Support (SPSS) Statistics 27.0 software.